Cathode Materials

DOI: 10.1002/anie.201005428

Electrospinning of Highly Electroactive Carbon-Coated Single-Crystalline $LiFePO_4$ Nanowires

Changbao Zhu, Yan Yu, Lin Gu,* Katja Weichert, and Joachim Maier**

Among the candidates for cathode materials in lithium-based batteries, the olivine-structured $LiFePO_4$, as first proposed by Goodenough and co-workers in 1997,[1] has attracted much interest owing to its significant advantages, including high theoretical capacity (170 mA h g^{-1}), acceptable operating voltage (3.4 V vs. Li^+/Li), environmental benignity, high safety, and low cost.[2–7]

Notwithstanding the numerous advantages, the main weakness of $LiFePO_4$ is its intrinsically sluggish mass and charge transport,[8–12] which was demonstrated by recent work on $LiFePO_4$ single crystals.[13,14] Therefore intensive attempts have been made to overcome its ionic and electronic transport limitations, for example, by doping.[15–18] Owing to the opposite charge of the ionic (V_{Li}') and electronic carriers ($h^\bullet$), the effect of doping on chemical transport is not expected to be of massive impact.[14] Rather, reduction of the effective transport length[10,19–21] as well as assembly of clever conductive networks is more promising. For that purpose, coating of the $LiFePO_4$ particles with electronically conductive materials such as carbon,[22–26] silver,[27] or polymers[28] proved successful. Furthermore, particle coating by an ionically conducting glass[29] or by highly mixed conducting RuO_2[30] has been reported to be beneficial.

Besides network formation, morphology and shape of $LiFePO_4$ itself is a key issue. Numerous studies have investigated the development of synthetic methods to prepare nanometer-sized $LiFePO_4$ of different morphologies (e.g. spherical nanoparticles,[10,31] nanoplates,[32] nanoporous materials,[33] and nanowires[23,34]) and identified the most favorable ones in terms of performance.

Among the wide range of morphologies, nanowires are in principle promising, as they offer a better percolation behavior than particles.[35] However, to date there are only a few reports on the synthesis of $LiFePO_4$ nanowires: a hard template method was used by Lim et al.,[34] which is rather complicated since it includes postsynthesis treatment with HF or NaOH, which can dissolve or chemically react with $LiFePO_4$.[26] After synthesis, bundles of nanowires are obtained, and each wire is formed by agglomeration of individual particles.[34]

Another method is electrospinning, which is an inexpensive, simple, and versatile technique to obtain nanofibers[36,37] of different materials, such as polymers,[38] ceramic metal oxides,[39] or metals.[40] Depending on the individual experimental setup, a variety of porous, hollow, amorphous, and polycrystalline nanowires can be prepared.[36,39] In contrast, single-crystalline nanowires produced by electrospinning are quite rare.[41,42]

Recently, Hosono et al. synthesized carbon-coated $LiFePO_4$ nanowires as well as triaxial $LiFePO_4$ nanowires with a carbon nanotube core and a carbon shell by the electrospinning method.[43] The thickness of the $LiFePO_4$ nanowires (more than 500 nm up to 1 μm in diameter) constrains their performance, and much thinner nanowires are needed for practical use in lithium batteries.

Herein we report on in situ carbon-coated $LiFePO_4$ nanowires with diameters of around 100 nm produced by electrospinning. These nanowires are single-crystalline and show good electrochemical performance.

An aqueous precursor solution containing LiH_2PO_4, $Fe(NO_3)_3$, and poly(ethylene oxide) was used for the electrospinning process. Figure 1 a displays a schematic illustration of

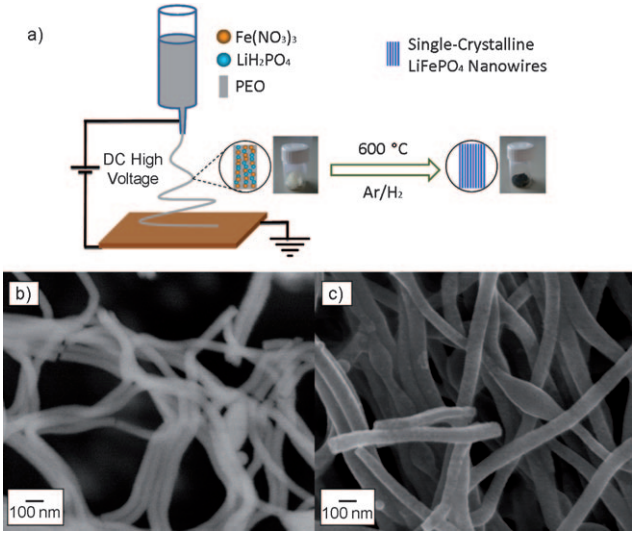

Figure 1. a) Schematic illustration of the electrospinning process. SEM images of b) as-prepared nanowires and c) SCNW-LFP heated at 600 °C for 2 h.

[*] C. Zhu, K. Weichert, Prof. Dr. J. Maier
Max Planck Institute for Solid State Research
Heisenbergstrasse 1, 70569 Stuttgart (Germany)
E-mail: S.Weiglein@fkf.mpg.de
Prof. Y. Yu
School of Materials Science and Engineering, Beihang University
Xueyuan Rd. 37#, Beijing, 100191 (P.R. China)
E-mail: yanyu@buaa.edu.cn
Prof. L. Gu
Beijing Laboratory for Electron Microscopy
Institute of Physics, Chinese Academy of Sciences
Beijing 100190 (P.R. China)
E-mail: l.gu@iphy.ac.cn

Supporting information for this article is available on the WWW under http://dx.doi.org/10.1002/anie.201005428.

the typical electrospinning setup. Long and continuous nanowires of fibrous morphology were obtained with thin and uniform diameters of about 100 nm, as shown by scanning electron microscopy (SEM; Figure 1b). Heating these as-prepared nanowires at 600°C for 2 h in H_2 (5 vol%)/Ar (95 vol%) atmosphere leads to decomposition of the polymer and the formation of carbon-coated $LiFePO_4$ nanowires with the same diameter (ca. 100 nm, Figure 1c). X-ray diffraction (XRD) analysis reveals crystalline, single-phase $LiFePO_4$ without detectable impurity phases (all peaks could be indexed according to ICDD card No. 01-081-1173, see the Supporting Information, Figure S1). Energy-dispersive X-ray (EDX) spectroscopy (Supporting Information, Figure S2) and transmission electron microscopy (TEM; Figure 2) confirm the presence of carbon, the content of which amounts to 6 wt%, as detected by elemental analysis.

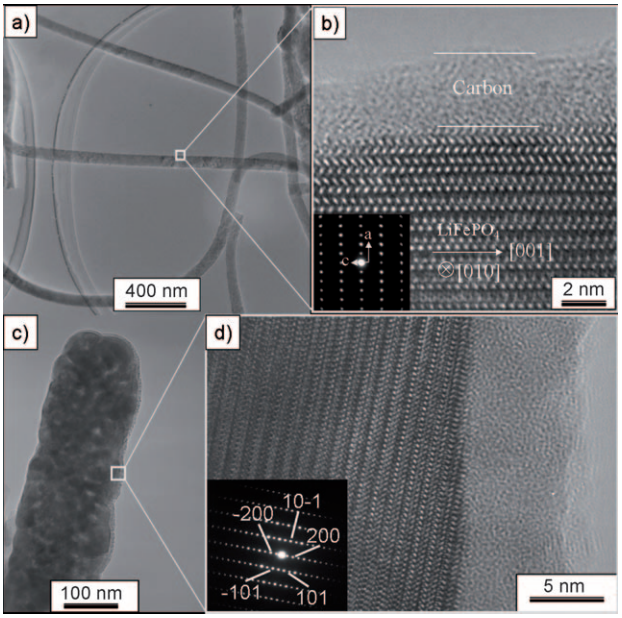

Figure 2. a) Overview TEM micrograph showing nanowires with a diameter of around 100 nm. b) Corresponding high-resolution (HR) TEM image from the marked region, inset: SAED pattern, region of 500 nm in diameter. The SAED pattern demonstrates that the growth direction is along the *c* axis (space group *Pnma*). c) TEM image of SCNW-LFP after 25 charge–discharge cycles. d) Corresponding HRTEM image from the marked region showing that the single-crystalline structure is maintained. Inset: SAED pattern, region of 500 nm in diameter.

The $LiFePO_4$ nanowires (denoted as SCNW-LFP) are uniform (Figure 2a) and single-crystalline, with the growth direction along the *c* axis (in the space group *Pnma*; Figure 2b). A preferred growth along the *c* axis was also observed for platelike $LiFePO_4$[44] and thumblike $LiMPO_4$ (M = Mn, Fe, Co, Ni)[45] nanocrystals. However, the main growth direction of large single crystals obtained by optical floating zone growth was along the *b* axis.[46] With the maximum diameter of the selected-area aperture being 500 nm, selected area electron diffraction (SAED) allowed us to acquire a pattern over the whole diameter of a single nanowire. It demonstrates entire single-crystallinity of the nanowire, as well as growth of the nanowire along the *c* direction (Figure 2b, inset). Note that inorganic nanowires produced by the electrospinning technique are usually polycrystalline. Only recently were single-crystalline metal oxide nanowires reported (V_2O_5[41] and Nb_2O_5[42]), and to our knowledge, there are no reports about single-crystalline nanowires of multielement materials such as $LiFePO_4$ prepared by this method. Even after repeated Li extraction and insertion during battery cycling, SCNW-LFP remains single-crystalline (Figure 2c,d).

The growth of SCNW-LFP along the *c* axis (Figure 2b) leads to short transport pathways along the *b* and *a* directions. As ion and electron transport along the *b* direction is much faster than for the *a* direction,[13,47–50] rapid lithium diffusion, namely along the *b* axis, is expected. (Whether or not transport in the *b* direction is perceptibly faster than along the *c* axis seems to depend on the degree of Li/Fe antisite disorder.[50]) Together with the well-ordered single-crystalline structure of the nanowires, this situation promotes fast Li insertion and extraction.[51]

Each nanowire is coated with an amorphous carbon layer of 2–5 nm thickness (Figure 2b), which suppresses aggregation[52–54] and is thin enough not to block Li transport. Individual SCNW-LFP nanowires are loosely connected with each other to form a three-dimensional network. Both the uniform carbon layer and the 3D connection ensure a continuous electronically conductive network, which together with the liquid electrolyte provides fast Li transport.

The electrochemical performance of SCNW-LFP is illustrated in Figure 3. Usually, 20% conductive carbon (Super-P) was used to prepare the electrode. For comparison, the rate capability of an electrode containing only 10% carbon is shown as well (Figure 3c,e). The cyclic voltammetry curve of the initial cycle reveals redox peaks centered at 3.52 (anodic peak) and 3.35 V (cathodic peak) and additionally a small shoulder[55–58] in the voltage range between 3.5 and 4.3 V. However, the shoulder gradually disappears in the subsequent cycles. The redox peaks correspond to Li^+ extraction and insertion from the $LiFePO_4$ framework, respectively.

The unique structure of SCNW-LFP results in fair discharge capacities and rate performance, for example, 169 (0.1 C), 162 (0.5 C), 150 (1 C), 114 (5 C), 93 mA h g^{-1} (10 C) at room temperature (Figure 3b). Note that the capacity at 0.1 C is close to the theoretical one of 170 mA h g^{-1}. Furthermore, SCNW-LFP exhibits excellent rate capability (Figure 3c) and capacity retention (Figure 3d). For instance, as much as 146 mA h g^{-1} can still be obtained after 100 cycles at 1 C discharge rate, which is 86% of the theoretical capacity (Figure 3d). During cycling, the morphology of SCNW-LFP is maintained (Figure 2c,d), thus promoting a good capacity retention. SCNW-LFP electrodes containing only 10% additional conductive carbon show a capacity drop of only 15–20 mA h g^{-1} compared to electrodes with 20% of carbon at each C rate, even at the highest rate of 10 C (Figure 3c). For comparison, commercially available $LiFePO_4$ (1 wt% carbon content) is shown to exhibit in general worse performance than SCNW-LFP (Figure 3c). The performance loss of

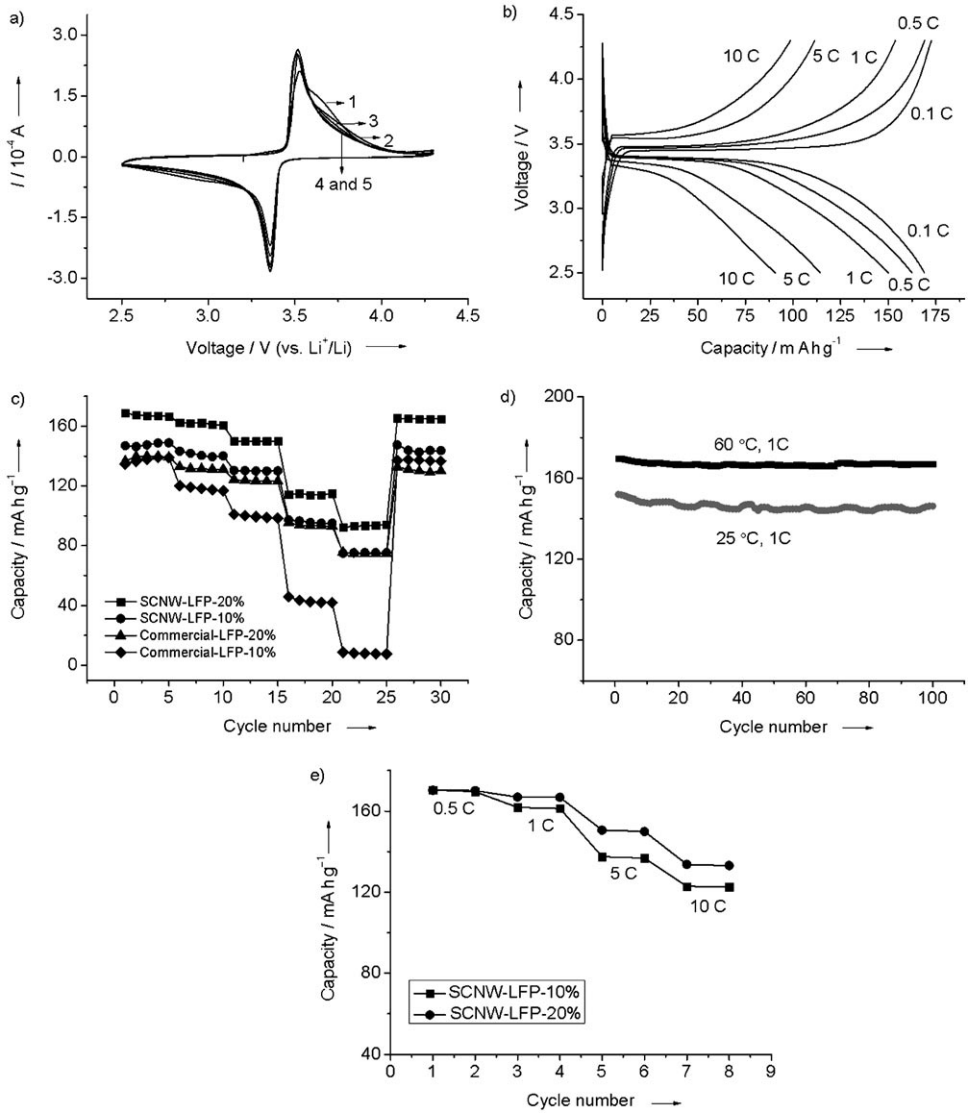

Figure 3. a) Cyclic voltammetry of SCNW-LFP, scan rate 0.1 $mV s^{-1}$. b) Charge and discharge profiles of SCNW-LFP at different C rates. c) Rate performance of SCNW-LFP and commercial $LiFePO_4$ with 10 and 20% additional conductive carbon. d) Cycling stability of SCNW-LFP at 1 C rate at room temperature and at 60°C. e) Rate performance of SCNW-LFP with 10 and 20% additional conductive carbon at 60°C.

commercial $LiFePO_4$ with 10% conductive carbon instead of 20% is much more severe than for SCNW-LFP, and at 10 C rate, the capacity becomes negligible (Figure 3c). The results show very clearly that in case of SCNW-LFP the amount of additional conductive carbon is of less impact on the performance than for the commercial carbon-coated $LiFePO_4$ particles. Therefore we think that in our nanowires an effective electronic wiring by the carbon coating of the active material is provided. However, as demonstrated by cyclic voltammetry, polarization of the SCNW-LFP electrode increases with decreasing carbon content as expected, owing to the reduction of electronic pathways to the current collector (Supporting Information, Figure S3).

We also examined the effect of elevated operating temperature on the electrochemical performance of SCNW-LFP. In general, the discharge capacity of the electrode increases at 60°C owing to improved kinetics. At a relatively low C rate (0.5 C), SCNW-LFP with both 10 and 20% additional conductive carbon delivers almost the theoretical capacity (170 $mA h g^{-1}$), and even at 10 C, capacity values of 134 (20% carbon) and 123 $mA h g^{-1}$ (10% carbon) were still obtained (Figure 3e). Furthermore, SCNW-LFP shows excellent cycling stability at elevated temperature (Figure 3d). For instance, almost the theoretical capacity was achieved at 1 C, and 98% capacity retention was obtained after 100 cycles at 60°C (Figure 3d).

The battery performance of SCNW-LFP is better than for the carbon-coated $LiFePO_4$ nanowires of Hosono et al. also produced by electrospinning. Even their triaxial $LiFePO_4$ nanowires with a carbon nanotube core, which improves the conductive network as well as the performance, show lower discharge capacities (160 (0.06 C), 130 (0.6 C), 80 $mA h g^{-1}$ (6 C))[43] than SCNW-LFP, which we attribute to the smaller thickness and well-ordered structure of our nanowires. (Our comparison is based on the reported discharge capacities, whereas parameters such as electrode thickness and loading were not given in the report by Hosono et al.[43] Note that these parameters can largely effect the battery performance.) Similar electrochemical behavior was observed in selected carbon-coated nanoparticles of 100 nm diameter[59] for which decisive parameters such as carbon content, thickness of the carbon layer, and transport lengths are comparable to our SCNW-LFP. However, the overpotentials of oxidation and reduction as derived from cyclic voltammetry are significantly higher for the nanoparticles ($\Delta V \approx 0.9$ V[59]) than for SCNW-LFP ($\Delta V \approx 0.23$ V, Figure 3a and Supporting Information, Figure S3).

In general, comparisons of $LiFePO_4$ electrodes are difficult, since parameters such as electrode thickness, loading, or carbon and electrode microstructure are not always reported or known. Beside a varying carbon content, these parameters influence the battery performance.[60,61]

Future work will focus on optimizing the electrospinning process to obtain nanowires with diameters of less than 50 nm

as well as nanoporous fibers with high surface area to further increase their performance.

In summary, we report on single-crystalline carbon-coated $LiFePO_4$ nanowires synthesized by the electrospinning method. These nanowires not only differ from reported analogues in crystallinity, but they are also substantially thinner. The nanowires grow along the *c* direction and feature a uniform and continuous carbon coating of moderate thickness. In this way, an efficient conductive network is formed, with very short diffusion lengths along the *b* axis leading to very good rate performance and cycling capability.

Experimental Section

Synthesis: LiH_2PO_4 (0.63 g, 6.1 mmol, Aldrich, $\geq 99\,\%$) and $Fe(NO_3)_3{\cdot}9H_2O$ (2.42 g, 6 mmol, Aldrich, $\geq 99.99\,\%$) were dissolved in water (30 mL, $\sigma = 0.2\ \mu S\,cm^{-1}$), and poly(ethylene oxide) (0.6 g, Aldrich, $M_v = 600\,000$, CAS: 25322-68-3) was added. The resultant precursor solution was poured into a syringe connected to a blunt cannula of 1.6 mm in diameter. The flow rate was approximately $10\ \mu L\,min^{-1}$, and a grounded stainless steel plate was placed 15 cm below the spinneret to collect the nanowires (Figure 1a). A high voltage of 15 kV was applied by a high-voltage power supply (Model HCE35-35000, FUG DC power source, Germany). The as-collected electrospun fibers were calcined in an Al_2O_3 crucible in a tube furnace at 600 °C for 2 h under H_2 (5 vol %)/Ar (95 vol %) atmosphere to obtain SCNW-LFP (heating rate $2\,°C\,min^{-1}$, cooling rate $5\,°C\,min^{-1}$). Commercial carbon-coated $LiFePO_4$ (particle size around 200 nm, carbon content about 1 wt %) was purchased from Advanced Lithium Electrochemistry Co., Ltd, Taiwan.

Structural and electrochemical characterization: XRD measurements were carried out with a Philips PW 3020 diffractometer using $Cu_{K\alpha}$ radiation. SEM was performed using a JEOL 6300F microscope operated at 5 keV. HRTEM and SAED were performed using a JEOL 2010F transmission electron microscope operated at 200 keV. The interpretable resolution defined by the contrast transfer function of the objective lens is 0.19 nm. EDX analysis was carried out using an Oxford system attached to a JEOL 2010F microscope. Carbon content was measured by combusting the material in a stream of oxygen with subsequent IR spectroscopic detection of the evolved CO_2.

SCNW-LFP or the commercial carbon-coated $LiFePO_4$ (70 (80) wt %), carbon black (20 (10) wt %, Super-P, Timcal), and poly(vinylidene fluoride) binder (10 wt %, Aldrich) in *N*-methylpyrrolidone were mixed into a homogeneous slurry (grounding with mortar and pestle for 10 min and subsequent magnetic stirring overnight in a closed beaker). The obtained slurry was pasted on Al foil using the doctor blade technique and was then dried in a vacuum oven for 12 h at 80 °C. Finally, round disks of 1 cm in diameter were cut; the loading of each was approximately $1.3\ mg\,cm^{-2}$ with an electrode thickness of around 50 μm. Electrochemical test cells (Swagelok-type) were assembled in an argon-filled glove box ($O_2 \leq$ 0.1 ppm, $H_2O \leq 3$ ppm) with the coated Al disk as working electrode, lithium metal foil as the counter and reference electrode, and 1 M solution of $LiPF_6$ in a 1:1 vol/vol mixture of ethylene carbonate and diethyl carbonate as the electrolyte (Novolyte technologies). Celgard 2400 film was used as separator. The batteries were charged and discharged galvanostatically in the fixed voltage window between 2.5 and 4.3 V on an Arbin MSTAT battery tester at room temperature (charge and discharge rate were the same). Cyclic voltammetry was performed with a Voltalab system (D21V032, Radiometer Analytical SAS, France) on Swagelok-type cells.

Received: August 30, 2010
Revised: February 14, 2011
Published online: May 30, 2011

Keywords: electrochemistry · electrospinning · lithium · nanotechnology · nanowires

[1] A. K. Padhi, K. S. Nanjundaswamy, J. B. Goodenough, *J. Electrochem. Soc.* **1997**, *144*, 1188.
[2] R. Dominko, M. Bele, J.-M. Goupil, M. Gaberscek, D. Hanzel, I. Arcon, J. Jamnik, *Chem. Mater.* **2007**, *19*, 2960.
[3] B. L. Ellis, W. R. M. Makahnouk, Y. Makimura, K. Toghill, L. F. Nazar, *Nat. Mater.* **2007**, *6*, 749.
[4] H. M. Xie, R. S. Wang, J. R. Ying, L. Y. Zhang, A. F. Jalbout, H. Y. Yu, G. L. Yang, X. M. Pan, Z. M. Su, *Adv. Mater.* **2006**, *18*, 2609.
[5] X. Wu, L. Jiang, F. Cao, Y. Guo, L. Wan, *Adv. Mater.* **2009**, *21*, 2710.
[6] S. F. Yang, Y. N. Song, P. Y. Zavalij, M. S. Whittingham, *Electrochem. Commun.* **2002**, *4*, 239.
[7] Y. Wang, Y. Wang, E. Hosono, K. Wang, H. Zhou, *Angew. Chem.* **2008**, *120*, 7571; *Angew. Chem. Int. Ed.* **2008**, *47*, 7461.
[8] N. Ravet, Y. Chouinard, J. F. Magnan, S. Besner, M. Gauthier, M. Armand, *J. Power Sources* **2001**, *97–98*, 503.
[9] P. S. Herle, B. Ellis, N. Coombs, L. F. Nazar, *Nat. Mater.* **2004**, *3*, 147.
[10] C. Delacourt, P. Poizot, S. Levasseur, C. Masquelier, *Electrochem. Solid-State Lett.* **2006**, *9*, A352.
[11] C. Delacourt, L. Laffont, R. Bouchet, C. Wurm, J. B. Leriche, M. Morcrette, J. M. Tarascon, C. Masquelier, *J. Electrochem. Soc.* **2005**, *152*, A913.
[12] K. S. Park, S. B. Schougaard, J. B. Goodenough, *Adv. Mater.* **2007**, *19*, 848.
[13] R. Amin, P. Balaya, J. Maier, *Electrochem. Solid-State Lett.* **2007**, *10*, A13.
[14] J. Maier, R. Amin, *J. Electrochem. Soc.* **2008**, *155*, A339.
[15] S. Y. Chung, J. T. Bloking, Y. M. Chiang, *Nat. Mater.* **2002**, *1*, 123.
[16] J. Yao, K. Konstantinov, G. X. Wang, H. K. Liu, *J. Solid State Electrochem.* **2007**, *11*, 177.
[17] N. Meethong, Y. H. Kao, S. A. Speakman, Y. M. Chiang, *Adv. Funct. Mater.* **2009**, *19*, 1060.
[18] M. Wagemaker, B. L. Ellis, D. Luetzenkirchen-Hecht, F. M. Mulder, L. F. Nazar, *Chem. Mater.* **2008**, *20*, 6313.
[19] N. Meethong, H. Y. S. Huang, S. A. Speakman, W. C. Carter, Y. M. Chiang, *Adv. Funct. Mater.* **2007**, *17*, 1115.
[20] C. Delacourt, P. Poizot, J. M. Tarascon, C. Masquelier, *Nat. Mater.* **2005**, *4*, 254.
[21] M. Gaberscek, R. Dominko, J. Jamnik, *Electrochem. Commun.* **2007**, *9*, 2778.
[22] R. Dominko, J. M. Goupil, M. Bele, M. Gaberscek, M. Remskar, D. Hanzel, J. Jamnik, *J. Electrochem. Soc.* **2005**, *152*, A858.
[23] C. R. Sides, F. Croce, V. Y. Young, C. R. Martin, B. Scrosati, *Electrochem. Solid-State Lett.* **2005**, *8*, A484.
[24] N. Ravet, J. B. Goodenough, S. Besner, M. Simoneau, P. Hovington, M. Armand, *The Electrochem. Soc. and The Electrochem. Soc. of Japan Meeting Abstracts* **1999**, *99–92*.
[25] R. Dominko, M. Bele, M. Gaberscek, M. Remskar, D. Hanzel, S. Pejovnik, *J. Electrochem. Soc.* **2005**, *152*, A607.
[26] C. M. Doherty, R. A. Caruso, B. M. Smarsly, P. Adelhelm, C. J. Drummond, *Chem. Mater.* **2009**, *21*, 5300.
[27] F. Croce, A. D. Epifanio, J. Hassoun, A. Deptula, T. Olczac, B. Scrosati, *Electrochem. Solid-State Lett.* **2002**, *5*, A47.
[28] Y. Huang, J. B. Goodenough, *Chem. Mater.* **2008**, *20*, 7237.
[29] B. Kang, G. Ceder, *Nature* **2009**, *458*, 190.
[30] Y. S. Hu, Y. G. Guo, R. Dominko, M. Gaberscek, J. Jamnik, J. Maier, *Adv. Mater.* **2007**, *19*, 1963.

[31] P. Gibot, M. Casas-Cabanas, L. Laffont, S. Levasseur, P. Carlach, S. Hamelet, J. M. Tarascon, C. Masquelier, *Nat. Mater.* **2008**, *7*, 741.
[32] K. Saravanan, M. V. Reddy, P. Balaya, H. Gong, B. V. R. Chowdari, J. J. Vittal, *J. Mater. Chem.* **2009**, *19*, 605.
[33] C. M. Doherty, R. A. Caruso, B. M. Smarsly, C. J. Drummond, *Chem. Mater.* **2009**, *21*, 2895.
[34] S. Lim, C. S. Yoon, J. Cho, *Chem. Mater.* **2008**, *20*, 4560.
[35] P. Bruce, B. Scrosati, J. M. Tarascon, *Angew. Chem.* **2008**, *120*, 2972; *Angew. Chem. Int. Ed.* **2008**, *47*, 2930.
[36] D. Li, Y. Xia, *Adv. Mater.* **2004**, *16*, 1151.
[37] J. J. Miao, M. Miyauchi, T. J. Simmons, J. S. Dordick, R. J. Linhardt, *J. Nanosci. Nanotechnol.* **2010**, *10*, 5507.
[38] A. Greiner, J. Wendorff, *Angew. Chem.* **2007**, *119*, 5770; *Angew. Chem. Int. Ed.* **2007**, *46*, 5670.
[39] W. Sigmund, J. Yuh, H. Park, V. Maneeratana, G. Pyrgiotakis, A. Daga, J. Taylor, J. C. Nino, *J. Am. Ceram. Soc.* **2006**, *89*, 395.
[40] Y. Yu, L. Gu, C. Wang, A. Dhanabalan, P. van Aken, J. Maier, *Angew. Chem.* **2009**, *121*, 6607; *Angew. Chem. Int. Ed.* **2009**, *48*, 6485.
[41] C. Ban, N. A. Chernova, M. S. Whittingham, *Electrochem. Commun.* **2009**, *11*, 522.
[42] A. L. Viet, M. V. Reddy, R. Jose, B. V. R. Chowdari, S. Ramakrishna, *J. Phys. Chem. C* **2009**, *114*, 664.
[43] E. Hosono, Y. Wang, N. Kida, M. Enomoto, N. Kojima, M. Okubo, H. Matsuda, Y. Saito, T. Kudo, I. Honma, H. Zhou, *ACS Appl. Mater. Interfaces* **2009**, *2*, 212.
[44] G. Y. Chen, X. Y. Song, T. J. Richardson, *Electrochem. Solid-State Lett.* **2006**, *9*, A295.
[45] A. V. Murugan, T. Muraliganth, P. J. Ferreira, A. Manthiram, *Inorg. Chem.* **2009**, *48*, 946.
[46] D. P. Chen, A. Maljuk, C. T. Lin, *J. Cryst. Growth* **2005**, *284*, 86.
[47] M. S. Islam, D. J. Driscoll, C. A. J. Fisher, P. R. Slater, *Chem. Mater.* **2005**, *17*, 5085.
[48] D. Morgan, A. Van der Ven, G. Ceder, *Electrochem. Solid-State Lett.* **2004**, *7*, A30.
[49] C. Ouyang, S. Shi, Z. Wang, X. Huang, L. Chen, *Phys. Rev. B* **2004**, *69*, 104303.
[50] R. Amin, J. Maier, P. Balaya, D. P. Chen, C. T. Lin, *Solid State Ionics* **2008**, *179*, 1683.
[51] Y. Ding, J. Xie, G. Cao, T. Zhu, H. Yu, X. Zhao, *Adv. Funct. Mater.* **2011**, *21*, 348.
[52] J. Jamnik, R. Dominko, B. Erjavec, M. Remskar, A. Pintar, M. Gaberscek, *Adv. Mater.* **2009**, *21*, 2715.
[53] K. F. Hsu, S. Y. Tsay, B. J. Hwang, *J. Mater. Chem.* **2004**, *14*, 2690.
[54] C. H. Mi, X. B. Zhao, G. S. Cao, J. P. Tu, *J. Electrochem. Soc.* **2005**, *152*, A483.
[55] Z. G. Lu, H. Cheng, M. F. Lo, C. Y. Chung, *Adv. Funct. Mater.* **2007**, *17*, 3885.
[56] Z. Chen, H. Zhu, W. Zhu, J. Zhang, Q. Li, *Trans. Nonferrous Met. Soc. China* **2011**, *20*, 614.
[57] L. Dimesso, S. Jacke, C. Spanheimer, W. Jaegermann, *J. Alloys Compd.* **2011**, *509*, 3777.
[58] S. Yu, G. Luo, Y. Luo, W. Liu, X. Yu, *Adv. Mater. Res.* **2011**, *160–162*, 1654.
[59] J. K. Kim, G. Cheruvally, J. H. Ahn, *J. Solid State Electrochem.* **2008**, *12*, 799.
[60] D. Y. W. Yu, K. Donoue, T. Inoue, M. Fujimoto, S. Fujitani, *J. Electrochem. Soc.* **2006**, *153*, A835.
[61] C. Fongy, A. C. Gaillot, S. Jouanneau, D. Guyomard, B. Lestriez, *J. Electrochem. Soc.* **2010**, *157*, A885.

